Interaction of Bacteriophage Lambda with Its Cell Surface Receptor: An in Vitro Study of Binding of the Viral Tail Protein gpJ to LamB (Maltoporin)[†]

Emir Berkane,[‡,§] Frank Orlik,[‡] Johannes F. Stegmeier,[‡] Alain Charbit,[||] Mathias Winterhalter,[§,⊥] and Roland Benz*[,‡]

Lehrstuhl für Biotechnologie, Biocenter of the University of Würzburg, Am Hubland, D-97074 Würzburg, Federal Republic of Germany, Institut de Pharmacologie et Biologie Structurale, 205 Route de Narbonne, F-31077 Toulouse, France, INSERM U-570, CHU Necker-Enfants Malades, F-75730 Paris Cedex 15, France, and School of Engineering and Science, International University of Bremen, D-28727 Bremen, Federal Republic of Germany

Received September 7, 2005; Revised Manuscript Received December 28, 2005

ABSTRACT: The cell surface receptor for bacteriophage Lambda is LamB (maltoporin). Responsible for phage binding to LamB is the C-terminal part, gpJ, of phage tail protein J. To study the interaction between LamB and gpJ, a chimera protein composed of maltose binding protein (MBP or MalE) connected to the C-terminal part of J (gpJ, amino acids 684−1131) of phage tail protein J of bacteriophage Lambda was expressed in *Escherichia coli* and purified to homogeneity. The interaction of the MBP−gpJ chimera protein with reconstituted LamB and its mutants LamB Y118G and the loop deletion mutant LamB Δ4+Δ6+Δ9v was studied using planar lipid bilayer membranes on a single-channel and multichannel level. Titration with the MBP−gpJ chimera blocked completely the ion current through reconstituted LamB when it was added to the cis side, the extracellular side of LamB with a half-saturation constant of ∼6 nM in 1 M KCl. Control experiments with LamB Δ4+Δ6+Δ9v from which all major external loops had been removed showed similar blocking, whereas MBP alone caused no visible effect. Direct conductance measurement with His_6−gpJ that contained a hexahistidyl tag (His_6 tag) at the N-terminal end of the protein for easy purification revealed no blocking of the ion current, requiring other measurements for the binding constant. However, when maltoporin was preincubated with His−gpJ, MBP−gpJ could not block the channel, which indicated that also His_6−gpJ bound to the channel. High-molecular mass bands on SDS−PAGE and Western blots, confirming the planar lipid bilayer experiment results, also demonstrated stable complex formation between His_6−gpJ and LamB or LamB mutants. The results revealed that phage Lambda binding includes not only the extracellular loops.

Two membranes surround Gram-negative bacteria (*1*). The outer membrane has an unusual lipid composition and a relatively simple protein pattern. The outer monolayer contains lipopolysaccharide (LPS) as its major or exclusive (in enteric bacteria) lipid, while the inner leaflet contains phospholipids [mostly phosphatidylethanolamine and small amounts of phosphatidylglycerol and cardiolipin (*2*)]. The outer membrane represents a very tight structure, which makes the Gram-negative bacteria resistant to host defense factors such as lysozyme and different leukocyte proteins (*3*). Furthermore, in enteric bacteria living in the intestinal tract of various organisms, the outer membrane represents a very effective barrier which protects the bacterial cells from the action of bile acid detergents and the degradation by digestive enzymes (*4*). Components of the outer membrane may serve as receptors for bacteriophages (*5*, *6*). Bacteriophages are viruses that attack bacteria and lyse sensitive bacterial cells (*7*−*9*). Although the different steps of infection with phages have been known for some time, the molecular mechanisms underlying infection of bacterial cells with phages remain unknown for the majority of them.

The first step of infection is always the binding of the phages to the host cell (*10*, *11*). Many of the proteins of the cell surface, including cell surface receptors, general diffusion porins, or substrate-specific channels and LPS, may act as receptors for phages (*12*, *13*). Porins and receptors form according to three-dimensional crystallography β-barrel cylinders with varying numbers of β-sheets; the general diffusion porins have 16, the specific porins 18, and the receptors 22 β-sheets (*14*−*20*). The interaction of phages with outer membrane proteins has been extensively studied in vitro for two systems: LamB of *Escherichia coli* as a receptor for phage Lambda (*21*, *22*) and FhuA of *E. coli* as a receptor for phage T5 (*23*, *24*). LamB is a trimeric protein of the outer membrane of Gram-negative bacteria and is part of the maltose uptake system (the *mal*-system) in *E. coli* and other members of family Enterobacteriaceae (*25*−*30*). The 18 β-sheets of LamB are connected at the periplasmic side by short turns and at the cell surface-exposed side by long

[†] Supported by grants of the Deutsche Forschungsgemeinschaft (Project Be 865/10), the Bayerisch-Französische Hochschulzentrum (Centre de Coopération Universitaire Franco-Bavarois), the Procope program of the Deutsche Akademische Austauschdienst (DAAD), and the French Ministère des Affaires Etrangères (MAE) and the Fonds der Chemischen Industrie.

* To whom correspondence should be addressed. Telephone: +49-(0)931-888-4501. Fax: +49-(0)931-888-4509. E-mail: roland.benz@mail.uni-wuerzburg.de.

[‡] Biocenter of the University of Würzburg.

[§] Institut de Pharmacologie et Biologie Structurale.

[||] INSERM U-570.

[⊥] International University of Bremen.

10.1021/bi051800v CCC: $33.50
Published on Web 02/03/2006

loops. Loop L3 stabilizes the β-barrel cylinder of the LamB monomers and restricts its size to ~5 Å × ~7 Å. The carbohydrate-binding site inside the channel, called the "greasy slide", is composed of six aromatic amino acids that line the channel lumen from the extracellular to the periplasmic opening (*16*, *17*). Some residues of the surface-exposed loops are involved in the transport of carbohydrates through the channel (*31*) but are also involved in bacteriophage Lambda binding (*21*). Structural data in combination with data obtained from LamB point mutations suggest that surface-exposed loops L4, L6, and L9 may be involved in binding of bacteriophage Lambda to LamB (*31*−*35*).

Bacteriophage Lambda has been studied well in the past (*36*−*38*). It is applied in molecular biology as a vehicle for gene transfer and could be used for the potential treatment of bacterial infections (*39*−*42*). Despite the broad interest, the precise mechanism of host cell infection is not understood. After the binding of the bacteriophage Lambda to the surface of the host cell, a yet unknown process triggers the injection of the viral DNA across both bacterial membranes (*43*). Two different states are involved in the formation of the complex between the bacteriophage Lambda and the LamB protein before and after ejection of the DNA, suggesting a conformational change of some viral proteins allowing the release of the DNA (*44*). Recently, phage tail protein J has been shown to bind bacteriophage Lambda to LamB (*22*). Interestingly, only the presence of LamB is required for the binding step and the transport of the viral DNA across the outer membrane (*44, 45*). The investigation of the interaction between LamB and protein J is necessary to improve our understanding of the infection mechanism of the host cell with the phage. Protein J has recently been cloned and partially purified after solubilization of inclusion bodies (*22*). Only the C-terminal extremity of protein J named gpJ seems to be necessary for the interaction with LamB (*46*). Indeed, fusion proteins carrying between 20 and 40% of the C-terminal part of protein J with the maltose binding protein (MBP−gpJ[1] proteins) are produced as soluble forms and bind to LamB on the surface of *E. coli* cells (*46*). In this paper, the in vitro interaction between the 40% C-terminal fragment of protein J (gpJ, amino acids 684−1131) and LamB was investigated using lipid bilayer experiments. Single-channel and multichannel experiments were performed with MBP−gpJ and with the His_6−gpJ fragment without the MBP part produced with a His_6 tag. The relevance of the external LamB loops was investigated using loop deletion mutant LamBΔ4+Δ6+Δ9v. SDS−PAGE and Western Blots confirmed the formation of stable complexes between LamB and MBP−gpJ and between LamB and His_6−gpJ.

MATERIALS AND METHODS

Isolation and Purification of LamB from Shigella sonnei, Wild-Type (WT) LamB of E. coli, and the LamB Mutants Y118G and Δ4+Δ6+Δ9v. WT LamB was isolated from TOP 10F′ (Invitrogen) cells and LamB from *S. sonnei* from the pop154 strain (*43*). The LamB-negative strain pop6510 (*thr leu thi metA lacY dex5 tonA supE recA srl::Tn10*) was the recipient for the pAC1-derived plasmid, which encodes the triple loop deletion mutant LamB Δ4+Δ6+Δ9v (*47*). The LamB-negative strain BL21(DE3)Omp8$^-$ was the recipient for the pAM117 modified plasmid, which encodes the mutant LamB Y118G, as described previously (*48*). Media and chemicals were described previously (*49*). The *E. coli* strains containing different plasmids were grown overnight at 37 °C (*47*). The cell cultures were harvested and passed three times through a French pressure cell at 10 MPa. Unbroken cells were removed by centrifugation. The cell envelopes were pelleted in an ultracentrifuge (Beckman Omega XL90) by centrifugation at 48 000 rpm for 60 min. The SDS-soluble material was removed from the envelopes by a SDS wash. The murein and associated proteins were suspended in a buffer containing 10 mM Tris-HCl (pH 7.5), 5 mM EDTA, 2 mM PMSF, and 2% (v/v) Triton X-100 to remove most of the proteins from the murein. The supernatant of a subsequent centrifugation step was applied to a starch column (amylose-Sepharose, New England Biolabs). The column was washed first with a buffer containing 20 mM Tris-HCl (pH 7.4), 200 mM NaCl, and 1% Triton X-100 to remove all unbound proteins. The column was eluted with the same buffer supplemented with 10% maltose to remove the bound LamB proteins from the column. Some of the fractions contained pure LamB protein or mutant LamB proteins in their trimeric form.

Expression and Purification of the MBP−gpJ Protein. Expression and purification of MBP−gpJ (MBP attached to amino acids 684−1132 of Lambda phage tail protein J) were performed as described previously (*46*). *E. coli* JM 501 cells were transformed with a pMal-c2X plasmid (New England Biolabs). Cells were grown in 200 mL of LB (Luria−Bertani) medium, which contained 1% glucose and 100 μg/mL ampicillin. When the OD_{600} reached 0.5, MBP−gpJ was induced with 0.3 mM IPTG and the cells were grown until the end of the exponential phase. Cells were washed twice with 200 mM NaCl and 20 mM Tris-HCl (pH 7.4) and resuspended in the same buffer supplemented with protease inhibitors (protease inhibitor cocktail P 8465, Sigma). Cells were disrupted (three times, 10 MPa) with the French pressure cell. After centrifugation (9000*g* for 30 min at 4 °C), the supernatant was applied to a starch column (amylose-Sepharose, New England Biolabs) and washed with the same buffer. Elution was performed with the same buffer supplemented with 10 mM maltose. The different fractions that eluted from the amylose column were highly enriched in MBP−gpJ (see Figure 1A). However, they contained impurities, probably degradation products of this protein. For further purification, MBP−gpJ was subjected to preparative SDS−PAGE. The band corresponding to MBP−gpJ (apparent molecular mass of 97 kDa) was cut out of the gel and was eluted overnight with a buffer containing 200 mM NaCl and 20 mM Tris-HCl (pH 8) in the cold. Purified MBP−gpJ remained active for ~2 weeks when it was stored at 4 °C or longer when it was frozen to −20 °C.

Construction of a Plasmid Encoding His_6−gpJ_(684−1132). The *gpJ* gene, encoding 40% of the C-terminal end of the J protein of the bacteriophage Lambda (amino acids 684−1132, called gpJ), was cut out from the *MalE-gpJ* gene (*46*) by using an *Eco*RI−*Hin*dIII digestion in tango buffer

[1] Abbreviations: LamB, maltoporin of *E. coli*; MBP, maltose binding protein (MalE) of *E. coli*; gpJ, C-terminal portion of J, the tail fiber protein of phage; MBP−gpJ, chimera protein consisting of MBP and gpJ (amino acids 684−1131 of J protein); His−gpJ, hexahistidyl gpJ protein; *G*, conductance (i.e., current divided by voltage).

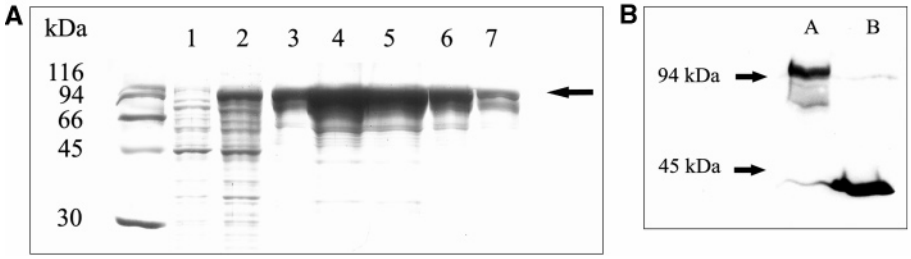

FIGURE 1: SDS−PAGE (10%) of the purification steps of MBP−gpJ. (A) In lane 1, 5 μL of total cell extract of induced *E. coli* cells was solubilized at 100 °C for 5 min in sample buffer. In lane 2, 5 μL of total cell extract of noninduced *E. coli* cells was solubilized at 100 °C for 5 min in sample buffer. The arrow shows the position of MBP−gpJ. In lanes 3−7 are the protein contents of different fractions of the amylose-Sepharose column after elution with buffer supplemented with maltose; 15 μL of the fractions were solubilized at 100 °C for 5 min in sample buffer. The gel was stained with Coomassie brilliant blue. (B) Western blot of MBP−gpJ and MBP (lanes A and B, respectively). The proteins were run on a 10% SDS−PAGE and blotted onto a nitrocellulose membrane. Rabbit antibodies against MBP were used in a 1/3000 dilution.

(Fermentas). The isolated fragment was inserted in a pBAD/His B multiple cloning site (Invitrogen Life Technologies) digested with the same restriction enzymes. *gpJ* was inserted between the *Eco*RI and *Hin*dIII digestion sites. Chemocompetent bacteria TOP 10F′ (Invitrogen) were transformed by the constructed plasmid encoding His_6−gpJ. Positive clones were selected on LB agar containing 100 μg/mL ampicillin. Sequencing of the newly obtained gene confirmed the DNA sequence of *gpJ* and revealed its coding for six additional histidines at its N-terminal end with the amino acid sequence MGGS**HHHHHH**GMASMTGGQQMGRDLYDDDDKD-PSSRSAAGTIWEF.

Expression and Purification of the His−gpJ Protein. Expression of the His_6−gpJ protein was performed as described by the manufacturer (Invitrogen life technologie pBAD/His B instruction manual version F). Cells were grown in 500 mL of LB medium supplemented with 100 μg/mL ampicillin at 37 °C. Induction with 0.2% arabinose (Roth) was performed when the OD_{600} equaled ≈0.4. Three hours after induction, cells were harvested by centrifugation (6000*g* for 15 min at 4 °C) and washed once in 100 mM NaCl and 20 mM Tris-HCl (pH 7.5). Cells were resuspended in the same buffer supplemented with protease inhibitors (protease inhibitor cocktail P8465, Sigma) and disrupted (three times, 10 MPa) with the French pressure cell. His_6−gpJ fusion protein was obtained as inclusion bodies attached to the cell envelope fraction as in the previous study, which means that the protein had to be renatured (*22*). For this, the pellet was solubilized in a buffer containing 200 mM NaCl, 8 M urea, and 20 mM Tris-HCl (pH 8). The supernatant of the subsequent centrifugation (6000*g* for 15 min at 4 °C) was incubated with Ni−NTA agarose (Qiagen) and was equilibrated with the same buffer overnight at 4 °C. The agarose was washed 10 times in 200 mM NaCl and 20 mM Tris-HCl (pH 8), supplemented with 20 mM imidazole (Roth) to completely remove the urea. For the elution of His_6−gpJ protein, the imidazole concentration was increased to 300 mM. The eluted protein was dialyzed against 200 mM NaCl and 20 mM Tris-HCl (pH 8) to remove imidazole, which interferes with the OD_{280} measurements for estimation of the protein concentration. His_6−gpJ was active for ∼2 weeks when it was stored at 4 °C and longer if it was kept frozen at −20 °C. Its stability under these conditions was approximately the same as that of the MBP−gpJ protein.

Immunodetection. After SDS−PAGE, proteins were transferred to a nitrocellulose membrane (Schleicher & Schuell, Protran) in Towbin buffer [25 mM Tris-HCl (pH 8.3), 152 mM glycine, and 20% methanol] for 45 min at 100 V and 350 mA (constant). The membrane was blocked with 5% nonfat dried milk powder in TBS-T buffer [20 mM Tris-HCl (pH 7.6), 140 mM NaCl, and 1% Tween 20]. Two kinds of immunodetection were performed: a detection using an anti-His_6 tag (a mouse Ig from Amersham Bioscience) and a detection using anti-MBP (an anti-MBP rabbit serum from New England Biolabs) as antibodies. The membrane was first incubated with the primary antibody in TBS-T (1/3000 dilution) and afterward with the secondary antibody (an anti-mouse or anti-rabbit immunoglobulin linked to horseradish peroxidase, both obtained from Amersham Bioscience) in TBS-T (1/3000 dilution) for 1 h at room temperature. Immunodetection was performed using the ECL Western Blotting Detection Reagents and Hyperfilm (Amersham Biosciences).

Bilayer Experiments. Black lipid bilayer membranes were formed from a 1% solution of diphytanoylphosphatidylcholine (Avanti Polar Lipids, Alabaster, AL) in *n*-decane as described previously (*50*). This instrumentation consisted of a Teflon chamber with two aqueous compartments filled with electrolyte (1 M KCl). The compartments are connected via a small circular hole with a surface area of ∼0.4 mm^2. The current was measured with a pair of Ag/AgCl electrodes with salt bridges connected in series with a voltage source and a current amplifier (Keithley 427 with a four-pole filter or a homemade current to voltage converter containing a Burr Brown operational amplifier with a three-pole filter). The amplified signal was monitored with a strip chart recorder to measure the membrane current. LamB was added from a concentrated stock solution to one side of the black lipid membranes (the cis side). Its reconstitution was observed by a stepwise increase in the membrane current. The temperature was kept at 20 °C and the membrane potential at 20 mV throughout.

In recent publications, the properties of specific channels have been studied in detail (*51*−*55*). Briefly, in a simple model, the stability constant for binding of the substrate to the binding site at the channel is determined by the relation $K = k_1/k_{-1}$. Furthermore, we assume that only one ligand molecule can bind to the binding site at a given time (*51*). The specific channel (given by P) is open when no ligand L is bound and closed when it is occupied to form the non- or low-conducting ligand−channel complex (PL):

$$P + L \underset{k_{-1}}{\overset{k_1 c}{\rightleftharpoons}} PL \quad (1)$$

The probability for an occupied binding site is p and, subsequently, $1 - p$ for a free site given by

$$1 - p = \frac{1}{1 + Kc} \quad (2)$$

The occupancy of the binding site is measured by the conductance $G(c) = I_m/V_m$, which is a function of the ligand concentration, c:

$$G(c) = G_{max}\frac{1}{Kc + 1} \quad (3)$$

where G_{max} is the membrane conductance before the start of the addition of the ligand to the aqueous phase. Equation 4 may also be written as

$$\frac{G_{max} - G(c)}{G_{max}} = \frac{Kc}{Kc + 1} \quad (4)$$

which means that the titration curves can be analyzed using the fit of eq 3 or by Lineweaver−Burke plots as shown in previous publications (*51*, *54*, *55*). The half-saturation constant, K_S, is given by the inverse stability constant $1/K$. The above-mentioned formalism is valid not only for the carbohydrate-induced block of LamB (*51*) but also for the clogging of the LamB channels by MBP−gpJ investigated here.

RESULTS

Purification of LamB and LamB Mutants. WT LamB of *E. coli*, LamB from *S. sonnei*, and the LamB mutants Δ4+Δ6+Δ9v and Y118G were obtained as described in Materials and Methods. The purity of the protein samples was checked by SDS−PAGE (data not shown). The trimers of the different proteins (with the exception of the LamB mutant Δ4+Δ6+Δ9v) had apparent molecular masses of ∼80 kDa and the monomers (after heating) ∼45 kDa. The molecular mass of LamB mutant Δ4+Δ6+Δ9v was somewhat smaller for the monomers (∼40 kDa) and the trimers (∼66 kDa) caused by the deletion of major surface-exposed loops L4 and L6 and a major part of loop L9 (*47*).

Purification of the MBP−gpJ Protein and His$_6$−gpJ. The MBP−gpJ protein was purified by affinity chromatography across an amylose-Sepharose column. After elution, the protein with an apparent molecular mass close to 97 kDa on SDS−PAGE (see Figure 1A) was not completely pure as described previously (*46*). Final purification was achieved by preparative SDS−PAGE. However, Western blots of the purified protein suggested that the protein still contained some minor contaminant protein that bound also the anti-MBP antibodies (see Figure 1B). The contaminant protein may be due to some intrinsic instability of the protein or its degradation by protease action, which could not be blocked by addition of protease inhibitors. Both MBP−gpJ preparations (eluted from the amylose column or obtained by preparative SDS−PAGE) interacted with LamB in the lipid bilayer experiments, indicating that there was no basic difference between the two MBP−gpJ preparations (see below). However, most experiments were performed using MBP−gpJ purified via preparative SDS−PAGE because of its higher purity. Attempts to release the gpJ part from the MBP−gpJ fusion protein by using protease factor Xa were unsuccessful. Therefore, *gpJ* was cloned in an expression vector that also encoded a hexahistidyl tag for easy protein purification at the N-terminal end of gpJ. The His$_6$−gpJ protein was found after induction in inclusion bodies. This means that its purification had to be performed under denaturing conditions using Ni−NTA agarose. After purification and renaturation, a pure and soluble protein with a molecular mass of ∼50 kDa was obtained (see Figure 2).

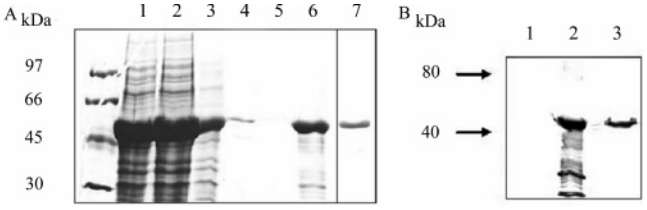

FIGURE 2: SDS−PAGE (10%) of the purification steps of His$_6$−gpJ. (A) In lane 1, 20 μL of solubilized inclusion bodies [in 8 M urea and 20 mM Tris-HCl (pH 8)] was dissolved at 100 °C in 10 μL of sample buffer. In lanes 2−5, supernatants of subsequent washing steps with 100 mM NaCl, 20 mM Tris-HCl (pH 8), and 20 μL of the solutions were dissolved at 100 °C in 10 μL of sample buffer. In lane 6, for the supernatant of the elution step using 100 mM NaCl and 20 mM Tris-HCl (pH 8) supplemented with 300 mM imidazole, 20 μL of the solution was dissolved at 100 °C in 10 μL of sample buffer. In lane 7, 3 μg of pure His$_6$−gpJ obtained by preparative SDS−PAGE was solubilized in 10 μL of sample buffer. The gel was stained with Coomassie brilliant blue. (B) Western blot using antibodies against His−gpJ. Cells expressing His$_6$-gpJ were disrupted and centrifuged: lane 1, analysis of the supernatant; lane 2, analysis of the pellet; and lane 3, analysis of His$_6$−gpJ purified by gel elution. The proteins were run on a 10% SDS−PAGE and blotted onto a nitrocellulose membrane. Mouse antibodies against the hexahistidyl tag were used at a dilution of 1/3000.

Effect of MBP−gpJ on the LamB Protein at the Single-Channel Level. Single-channel experiments were performed to investigate the interaction of MBP−gpJ with LamB in detail. LamB was added in a very small concentration (∼10^{-12} M) to the cis side of a black membrane formed of diphytanoylphosphatidylcholine and *n*-decane. After reconstitution of a few channels in the membrane, MBP−gpJ was added to the trans side of the membrane. Only in rare cases (∼10% of the experiments) was it possible to detect closure of single LamB channels by interaction with MBP−gpJ (data not shown). This is presumably caused by an ∼80−90% preferential orientation of reconstituted LamB. The surface-exposed parts of the trimers responsible for the interaction between LamB and gpJ are mainly localized on the cis side of the membrane (*56*).

Subsequently, MBP−gpJ was also added to the cis side of the membranes, resulting in a rapid decrease in the LamB-mediated conductance. Figure 3A shows an experiment of this type. After the insertion of one LamB trimer into the membrane, MBP−gpJ was added to the cis compartment of the cell at a concentration of 100 nM. The interaction between both proteins resulted in a complete block of the ionic current through WT LamB. Only some occasional flickers of the channels were observed, indicating that the lifetime of the open state was very small. In another series of experiments, LamB and MBP−gpJ were mixed at approximately equal concentrations (100 nM). Then the mixture was added to the cis side of the cell at a concentration suf-

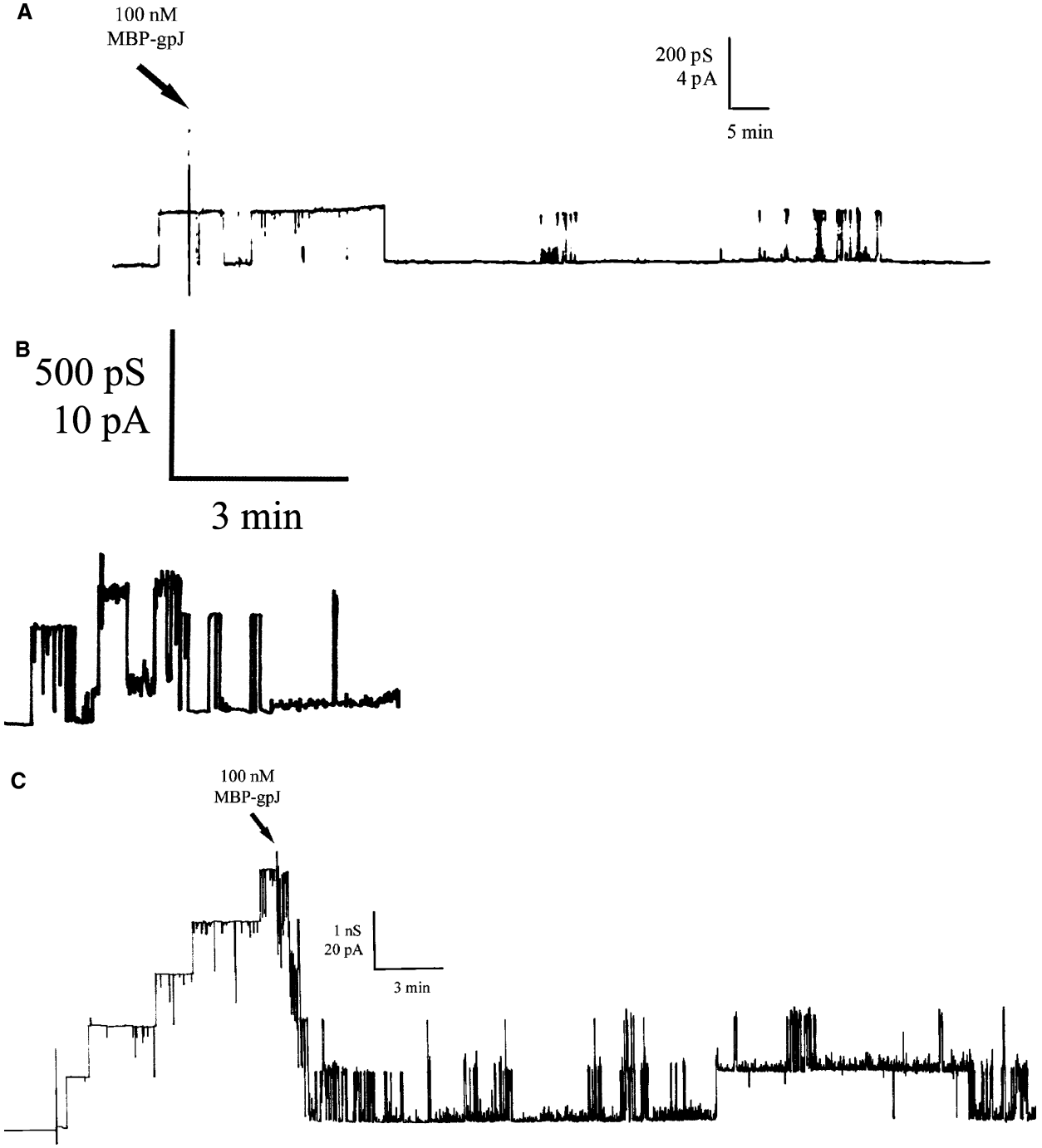

FIGURE 3: Effect of MBP−gpJ on LamB and LamB mutant Y118G measured at the single-channel level. (A) MBP−gpJ was added at a concentration of 100 nM to the cis side of a membrane (arrow) after the reconstitution of one wild-type LamB channel. The channel displayed an open substate (open) and gated to a closed level (closed). Zero (0) represents the zero current level. Note that the channel opened for only a short time. (B) LamB and MBP−gpJ were mixed at equal concentrations. The mixture was added at a concentration of ~100 nM to the cis side of a black membrane ~15 min before the recording started. Note that under these conditions only a small number of rapid switching channels was observed. (C) MBP−gpJ was added at a concentration of 100 nM to the cis side of a membrane (arrow) after the reconstitution of five Y118G mutant LamB channels. The channels close and show rapid flickering. The membranes were formed from diphytanoylphosphatidylcholine and *n*-decane. The aqueous phase contained 1 M KCl and $\sim 10^{-14}$ M LamB or LamB Y118G mutant. The applied voltage was 20 mV at the cis side, and $T = 20$ °C.

ficiently high to result in the reconstitution of more that 1000 channels in the absence of MBP−gpJ. In contrast, Figure 3B demonstrates that only a small number of channels formed under these conditions because the reconstitution was rare for the LamB−MBP−gpJ complex or due to a block of most of the LamB channels. The channels that could electrically be detected under these conditions showed the same open and closing kinetics observed by the block of LamB by MBP−gpJ. It is noteworthy that the small amount of SDS eluted together with MBP−gpJ from preparative gels did not interfere with the results described above. Control experiments with SDS alone added to the same concentration as with MBP−gpJ did not interfere with the LamB-mediated conductance. Furthermore, the addition of 0.01% SDS to the aqueous phase did not interfere with binding of MBP−gpJ to LamB.

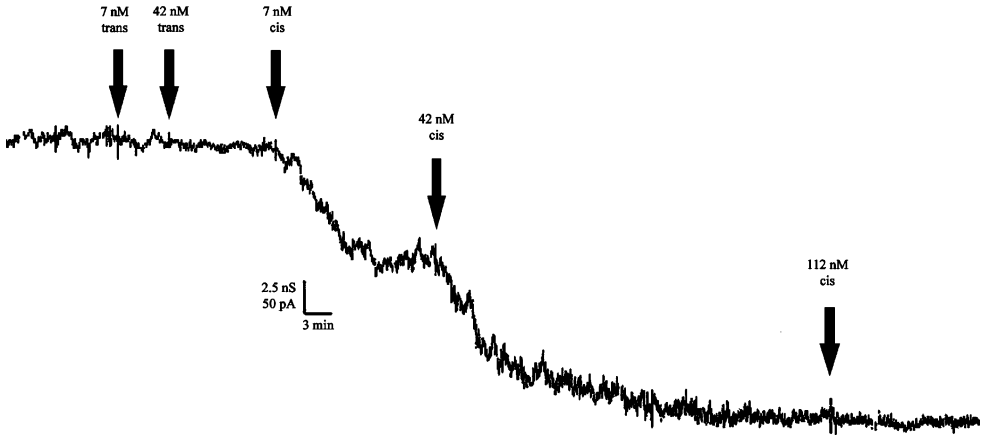

FIGURE 4: Titration of LamB-mediated conductance with MBP−gpJ. LamB was added to the cis side of a black diphytanoylphosphatidylcholine/*n*-decane membrane at a concentration of 10^{-12} M. The experiment started when ~150 channels were reconstituted in the membrane. Increasing concentrations of MBP−gpJ were added first to the trans side (arrows) and then to the cis side of the cell (arrows). The aqueous phase contained 1 M KCl and $\sim 10^{-12}$ M LamB. The applied voltage was 20 mV at the cis side, and $T = 20$ °C.

Y118G is a LamB mutant in which tyrosine 118 localized in the central constriction of the channel was replaced with glycine (*48*). This mutant has a single-channel conductance of ~900 pS in 1 M KCl compared to a value of 150 pS for WT LamB, allowing the study of channel blocking in more detail. For example, in Figure 3C after the reconstitution of five LamB Y118G mutant channels, 100 nM MBP−gpJ was added to the cis side. The interaction between LamB Y118G and MBP−gpJ also resulted in a complete block of the channels. The kinetics of channel closure was approximately the same as that measured above for WT LamB. The interaction between LamB of *S. sonnei* and MBP−gpJ was very similar to that exhibited by LamB of *E. coli* (data not shown). The results of Figure 3C and similar experiments demonstrated that the binding of MBP−gpJ to LamB resulted in a complete block of the trimers in a single step despite the fact that a trimer contains three individual channels that can be blocked independently of one another with carbohydrates (*51*, *52*, *57*). This means that the channels switched between a fully open and a fully closed state, caused by the binding of the MBP−gpJ protein (see Figure 3). However, the closed channels also exhibited some flickers as seen in Figure 3. Preliminary studies of the MBP−gpJ-mediated block of the LamB channels support this view. Fast Fourier transformation of the current noise demonstrated that the power density spectra were controlled by a Lorentzian function, indicating that a chemical reaction is involved in the binding process (E. Berkane, F. Orlik, M. Winterhalter, and R. Benz, unpublished results). Power density spectra of the noise of open channels can be described by a $1/f$ function (*52*, *58*, *59*). The experiments shown in Figure 3 demonstrated that MBP−gpJ blocks the LamB channel but did not induce channels by its own into the lipid bilayers because only a decrease in membrane conductance was observed (no increase). The latter would have been expected for the homology of protein J with proteins pb2 and p33 of phages T5 and T1, respectively. At least pb2 has been demonstrated to be a channel-forming component (*60*). However, control experiments with MBP−gpJ alone or with His_6−gpJ alone (see below) did not provide any indication that both proteins could be channel formers in lipid bilayer experiments.

Evaluation of the Stability Constant for Binding of MBP−gpJ to LamB. Titration measurements were performed with membranes that contained many LamB channels (aqueous concentration of LamB of ~100 nM) to quantify the binding of MBP−gpJ to LamB. Figure 4 shows such an experiment. LamB was added to the cis side of a membrane. When the reconstitution of channels reached an equilibrium, MBP−gpJ was added at increasing concentrations to the trans side and the cis side of the membrane. MBP−gpJ was first added only to the trans side of the membrane at concentrations of 7 and 42 nM (left side arrows in Figure 4). This resulted in an only insignificant decrease in the membrane conductance. The decrease was in this and similar experiments at maximum ~15%, corresponding to a minor fraction of channels, which exposed their cell surface side to the trans side (*56*). Then MBP−gpJ was added to the cis side while the mixture was being stirred to allow equilibration (right side arrows, 7 and 42 nM MBP−gpJ). The LamB-induced conductance decreased in a dose-dependent manner. The titration experiment of Figure 4 and similar measurements were analyzed as previously performed with the carbohydrate binding channels of Gram-negative bacteria (*51*, *61*) using a fit of the data using eq 3 or Lineweaver−Burke plots (eq 4).

Figure 5 shows the fit of the data of Figure 4 and similar experiments using eq 3 (□and —). The stability constant for binding of MBP−gpJ to LamB was $\sim 8 \times 10^7$ M^{-1}. The half-saturation constant, K_S, is given by the inverse binding constant, $1/K$, and was ~13 nM. Unfortunately, the fit of the titration data of Figure 4 and similar experiments using eq 3 was not satisfactory as the solid line in Figure 5 indicated. This could be explained either by the assumption that the LamB channels did not close completely when MBP−gpJ was bound, which is in contrast to the results of Figure 3, or by the assumption that some channels did not react to MBP−gpJ (see the Discussion). To account for this, we modified eq 4 accordingly:

$$\frac{G_{max} - G(c)}{G_{max} - G_{\infty}} = \frac{Kc}{Kc + 1} \qquad (5)$$

where G_∞ is the conductance at very high MBP−gpJ concentrations, i.e., the fraction of the conductance that did not seem to be blocked by MBP−gpJ. Figure 5 also shows the fit of the titration data using eq 5 (● and − − −). It was much better and yielded a stability constant, K, of ~1.7 ×

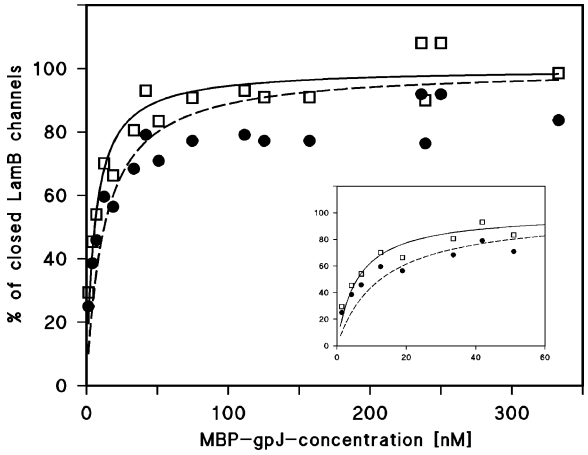

FIGURE 5: Fit of the results of the titration experiment shown in Figure 4 and of similar experiments with eq 5 (□ and —) or eq 6 (● and − − −). The fit of the data using eq 4 yielded the following parameters: $K_S = 21 \pm 1.9$ nM. The fit using eq 5 yielded the following ones: $K_S = 6.2 \pm 0.08$ nM, $G_\infty = 85\%$ of G_{max}. For further explanations, see the text. This figure represents the results of three experiments performed in 1 M KCl. The applied voltage was 20 mV at the cis side, and $T = 20$ °C.

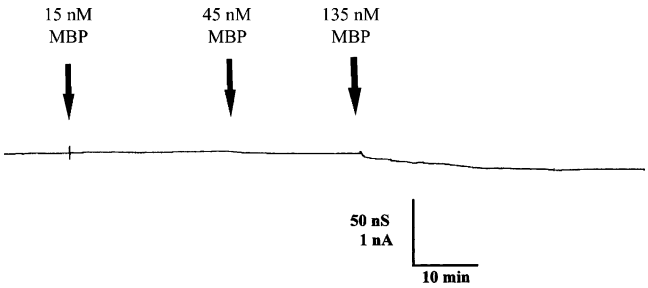

FIGURE 6: Effect of MBP on LamB-mediated membrane conductance. LamB was added to the cis side of a black diphytanoylphosphatidylcholine/*n*-decane membrane at a concentration of 10^{-12} M. The experiment started when ~2000 channels were reconstituted in the membrane. Increasing concentrations of MBP were added to the cis side of the membrane (arrows). The aqueous phase contained 1 M KCl. The applied voltage was 20 mV at the cis side, and $T = 20$ °C. Note that the addition of MBP led to an only insignificant decay in membrane conductance.

10^8 M^{-1} ($K_S = 5.8$ nM) for several titration experiments of the same type. On average, 85 ± 3% of the total conductance was blocked by MBP−gpJ.

Similar experiments were performed with LamB of *S. sonnei* and LamB mutant Y118G. These experiments yielded very similar stability constants for binding of MBP−gpJ to LamB (data not shown).

To investigate the effect of ionic strength on binding of MBP−gpJ to LamB, the salt concentration was varied. Most titration experiments were performed in 1 M KCl but some also in 0.1 M KCl. The stability constant was in these experiments approximately the same, indicating that the ionic strength had a minor influence if any on the interaction between MBP−gpJ and LamB.

The experiments described above suggest a high-affinity binding of MBP−gpJ to LamB. In a previous study, it has been suggested that MBP modulates LamB function in a voltage-dependent manner in reconstitution experiments with lipid bilayer membranes (*62*). The MBP-mediated effect of MBP on LamB was absent in other in vivo and in vitro studies (*28*, *63*). In agreement with these studies, our control experiments did not show any significant effect of MBP on

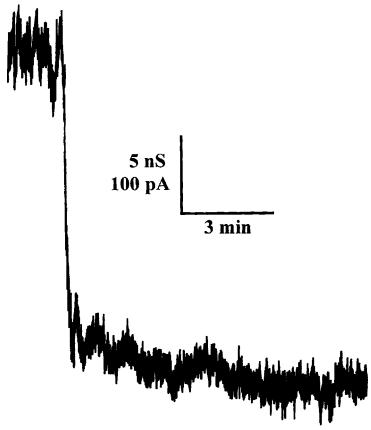

FIGURE 7: Effect of MBP−gpJ on the conductance mediated by LamB mutant Δ4+Δ6+Δ9v. The mutant was added to the cis side of a black diphytanoylphosphatidylcholine/*n*-decane membrane at a concentration of 10^{-12} M. When ~260 channels were reconstituted in the membrane, MBP−gpJ was added to the cis side of the membrane at a concentration of 100 nM (arrow). The aqueous phase contained 1 M KCl. The applied voltage was 20 mV at the cis side, and $T = 20$ °C.

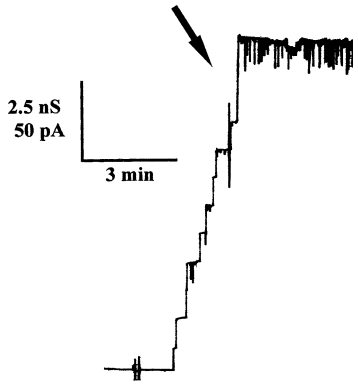

FIGURE 8: Effect of His_6−gpJ on LamB mutant Y118G measured on the single-channel level. His_6−gpJ was added at a concentration of 50 μM to the cis side of a diphytanoylphosphatidylcholine/*n*-decane membrane (arrow) after the reconstitution of nine Y118G mutant LamB channels. The aqueous phase contained 1 M KCl. The applied voltage was 20 mV at the cis side, and $T = 20$ °C. Note that the reconstitution of further channels stopped shortly after the addition of His_6−gpJ and that the open channels show rapid flickering.

LamB-mediated membrane conductance at concentrations up to 135 nM (see Figure 6). This result suggests that the gpJ part of the chimera protein is responsible for the MBP−gpJ-promoted block of the LamB channels.

Effect of Mg^{2+} and EDTA on the Complex between LamB and MBP−gpJ. EDTA prevents the formation of the complex between the bacteriophage Lambda and LamB, whereas Mg^{2+} increases the affinity of the phage for its receptor (*64*). Reconstitution experiments were performed to study the effect of both compounds on the interaction of MBP−gpJ with LamB. After reconstitution of a few channels into the membrane, the decrease in the LamB-mediated conductance was still possible when small amounts of MBP−gpJ were added to the cis side of the membrane. A final EDTA concentration as high as 20 mM did not change this result, indicating that EDTA did not prevent complex formation in vitro. Similarly, experiments performed in the presence of Mg^{2+} (final concentration from 5 to 20 mM) did not show any significant effect on the binding of MBP−gpJ to LamB.

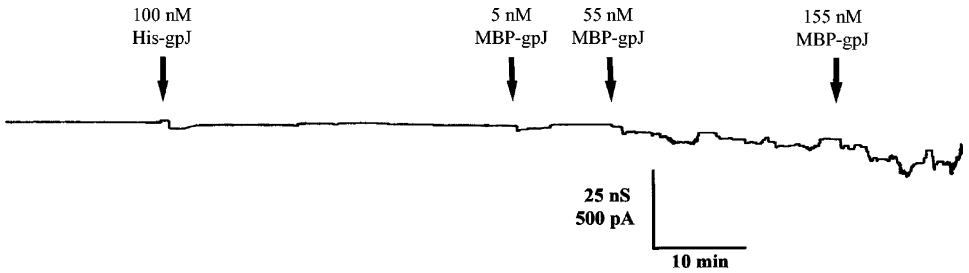

FIGURE 9: Effect of His_6−gpJ on the titration of LamB-mediated conductance with MBP−gpJ. LamB was added to the cis side of a black diphytanoylphosphatidylcholine/*n*-decane membrane at a concentration of 10^{-12} M. The experiment started when ~250 LamB channels were reconstituted in the membrane. First, His_6−gpJ was added to the cis side of the membrane at a concentration of 100 nM while the mixture was being stirred to allow equilibration (left side arrow). Approximately 30 min later, MBP−gpJ was added to the cis side at concentrations increasing from 5 to 155 nM (arrows). The aqueous phase contained 1 M KCl. The applied voltage was 20 mV at the cis side, and $T = 20$ °C. Note that the addition of His_6−gpJ prevented the block of the LamB channels by MBP−gpJ.

These results indicated that the presence of Mg^{2+} ions is not required for the formation of the complex between LamB and the MBP−gpJ protein.

Binding of MBP−gpJ to LamB Δ4+Δ6+Δ9v. Effects of mutations of LamB performed in the past suggested that amino acids localized on outer loops L4, L6, and L9 are involved in the infection of *E. coli* cells with bacteriophage Lambda (*31*−*35*, *65*). In vivo, this mutant does not serve as a receptor for bacteriophage Lambda (*47*). To investigate if these surface-exposed loops are involved in the binding of MBP−gpJ to LamB, we reconstituted LamB Δ4+Δ6+Δ9v. Channels formed by this mutant were rather unstable, resulting in a slow decrease following the initial rapid reconstitution of channels. This means that precise information about the stability constant for binding of MBP−gpJ to this mutant was not available. However, it was possible to demonstrate that MBP−gpJ could still block ion transport through LamB Δ4+Δ6+Δ9v. Figure 7 shows an experiment in which 100 nM MBP−gpJ was added to the cis side of a membrane containing ~260 LamB Δ4+Δ6+Δ9v channels. The addition resulted in a significant and rapid decrease in the conductance of LamB (see Figure 7). However, the addition of 100 nM MBP−gpJ did not result in a complete block of the LamB-mediated conductance as compared to that of WT LamB. This result suggests that the interaction of the MBP−gpJ protein with LamB is not localized within surface loops L4 and L6 and part of loop L9 alone.

Effect of His_6−gpJ on LamB Conductance and MBP−gpJ Binding. Experiments were also performed with His_6−gpJ to separate the effect of the protein J fragment (amino acids 684−1132) from that of MBP−gpJ on the LamB-mediated membrane conductance. Figure 8 shows such a measurement. His_6−gpJ (100 nM) was added to the cis side of a lipid bilayer membrane after reconstitution of nine LamB channels (arrow in Figure 8). Interestingly, unlike that observed in the experiments with MBP−gpJ, no decrease in LamB-mediated conductance occurred. On the other hand, it was not possible to detect any further increase in conductance, which means reconstitution of channels is inhibited after addition of His_6−gpJ to the cis side of the membrane. Furthermore, some increase in the level of channel flickering was observed (see Figure 8). This result indicated that interaction may exist between LamB and His_6−gpJ, but it did not lead to channel closure. These observations suggest that His_6−gpJ is not a channel-forming component; otherwise, its addition should have resulted in an increase in conductance (see below and the Discussion).

More direct proof of the interaction of His_6−gpJ with LamB was achieved in the experiment shown in Figure 9. His_6−gpJ was first added at a concentration of 100 nM (left side arrow in Figure 9) to the cis side of a membrane containing many LamB channels while the mixture was being stirred to allow equilibration. No channel closure or channel opening was observed as described above. Approximately 40 min after the addition of His_6−gpJ, MBP−gpJ was added to the same side of the membrane in concentrations increasing from 5 to 155 nM that are sufficient for channel closure (arrows in Figure 9). MBP−gpJ had an only small effect on the LamB-mediated membrane conductance. Only an insignificant decrease was observed at the very high MBP−gpJ concentrations of 55 and 155 nM, which without His_6−gpJ lead to the almost complete block of LamB channels. This result, observed in several independent experiments, confirmed the binding of His_6−gpJ to LamB, which prevented the binding of the MBP−gpJ protein and subsequent channel block.

Effect of the Complex between LamB and His_6−gpJ on Maltopentaose Transport. The results presented above indicate that His_6−gpJ binds to LamB. Ion flux seems still to be possible when His_6−gpJ is bound to LamB. In additional experiments, we investigated if the transport of carbohydrates through LamB was still possible when His_6−gpJ was bound. For this, LamB was reconstituted in lipid bilayer membranes. When the rate of incorporation had slowed considerably, His_6−gpJ was added to the cis side of the membrane while the mixture was being stirred to allow equilibration. After some period of incubation, a titration experiment was performed in which increasing amounts of maltopentaose were added only to the cis side of the membrane because maltopentaose binding should be influenced only from the cis side where His_6−gpJ is bound. Table 1 shows the results. The stability constant for maltopentaose binding was ~630 M^{-1} (corresponding to a half-saturation constant of 1.6 mM) for LamB mutant Y118G. Control experiments were also performed with LamB mutant Y118G alone to allow a meaningful comparison of the results. For the addition of maltopentaose to the cis side of the Y118G mutant, a binding constant of 770 M^{-1} (half-saturation constant of 1.3 mM) was obtained. This means that the binding of maltopentaose was not significantly modified, indicating that the binding of His_6−gpJ did not hinder the access of carbohydrates to the channels.

Detection of the Complexes among LamB, LamB Δ4+Δ6+Δ9v, and His_6−gpJ by SDS−PAGE and Western

Table 1: Stability Constants for Binding of Maltopentaose to the LamB Y118G Mutant in Presence or Absence of the His_6−gpJ Protein[a]

	control (without His_6−gpJ)	with 100 nM His_6−gpJ
K (M^{-1})	770 ± 100	630 ± 200
K_S (mM)	1.3 ± 0.2	1.6 ± 0.5

[a] The membranes were formed from diphytanoylphosphatidylcholine and *n*-decane. The aqueous phase contained 1 M KCl and ∼500 ng/mL LamB Y118G mutant added to the cis side of the membrane only. K was derived from titration experiments similar to those described previously (*28*) with the exception that maltopentaose was added to only the cis side of the membrane. For the experiment with His_6−gpJ, 100 nM His_6−gpJ was added first to the cis side of the membrane after the end of the reconstitution of LamB Y118G channels in the membrane, and then the titration with increasing maltopentaose concentrations was performed. The data represent means ± the standard deviation of at least three individual titration experiments. The applied voltage was 20 mV at the cis side, and T = 20 °C.

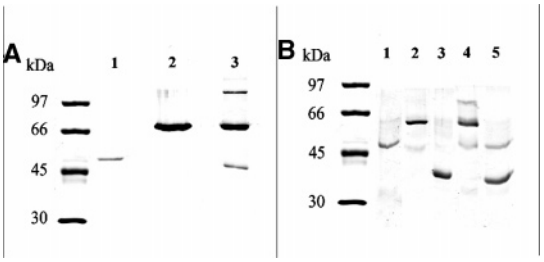

FIGURE 10: SDS−PAGE (10%) of complexes between wild-type LamB or mutant LamB Δ4+Δ6+Δ9v with His_6−gpJ. The gels were stained with Coomassie brilliant blue. (A) Lane 1: 5 μg of purified His_6−gpJ solubilized at 30 °C for 5 min in 5 μL of sample buffer. Lane 2: 5 μg of purified wild-type LamB solubilized at 30 °C for 5 min in 5 μL of sample buffer. Lane 3: 5 μg of purified wild-type LamB mixed with 5 μg of purified His_6−gpJ solubilized at 30 °C for 5 min in 5 μL of sample buffer. (B) Lane 1: 5 μg of purified His_6−gpJ solubilized at 30 °C for 5 min in 5 μL of sample buffer. Lane 2: 3 μg of purified LamB Δ4+Δ6+Δ9v solubilized at 30 °C for 5 min in 5 μL of sample buffer. Lane 3: 3 μg of purified LamB Δ4+Δ6+Δ9v solubilized at 100 °C for 5 min in 5 μL of sample buffer. Lane 4: 3 μg of purified LamB Δ4+Δ6+Δ9v mixed with 5 μg of purified His_6−gpJ solubilized at 30 °C for 5 min in 5 μL of sample buffer. Lane 5: 3 μg of purified LamB Δ4+Δ6+Δ9v and 5 μg of purified His_6−gpJ solubilized at 100 °C for 5 min in 5 μL of sample buffer.

Blotting. To demonstrate the possible formation of a complex of LamB, LamB Δ4+Δ6+Δ9v, and His_6−gpJ, trimers of WT Lamb, and mixtures of both, we performed SDS−PAGE with the single components and possible complexes (see Figure 10A, lanes 1−3). Lane 1 shows the pure His_6−gpJ (apparent molecular mass of 55 kDa). Lane 2 corresponds to the pure LamB trimers (75 kDa). Surprisingly, lane 3 exhibited three bands when LamB and His_6−gpJ were mixed together at approximately equal amounts. Two bands could easily be identified because they corresponded to LamB trimers and His_6−gpJ. The third band of lane 3 had an apparent molecular mass of ∼100 kDa and corresponded to the LamB−His_6−gpJ complex. Additional experiments with His_6−gpJ and LamB mutant Δ4+Δ6+Δ9v revealed that these proteins formed also a complex (Figure 10B, lane 4). Furthermore, the complex was absent when both LamB mutant Δ4+Δ6+Δ9v and His_6−gpJ were first mixed at 30 °C and then boiled (Figure 10B, lane 5). This result suggests that complexes formed only when LamB was in its trimeric form. Boiling of His_6−gpJ did not inhibit complex formation (see below).

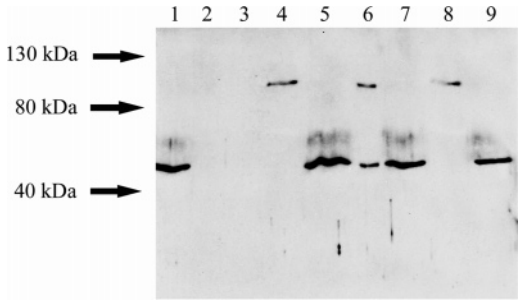

FIGURE 11: Western blot to detect complexes of LamB and LamB mutant Δ4+Δ6+Δ9v with His_6−gpJ. The proteins were run on a 10% SDS−PAGE gel and blotted onto a nitrocellulose membrane. Mouse antibodies against the hexahistidyl tag were used at a dilution of 1/3000. Lane 1: His-gpJ, solubilized at 30 °C. Lane 2: wild-type LamB solubilized at 30 °C. Lane 3: LamB mutant Δ4+Δ6+Δ9v, solubilized at 30 °C. Lane 4: wild-type LamB mixed with His_6−gpJ solubilized at 30 °C. Lane 5: wild-type LamB mixed with His_6−gpJ at 30 °C and then boiled at 100 °C. Lane 6: LamB Δ4+Δ6+Δ9v mixed with His−gpJ and solubilized at 30 °C. Lane 7: LamB mutant Δ4+Δ6+Δ9v mixed with His−gpJ at 30 °C and then boiled at 100 °C. Lane 8: LamB solubilized at 30 °C mixed with His_6−gpJ solubilized at 100 °C. Lane 9: wild-type LamB solubilized at 100 °C mixed with His−gpJ, solubilized at 30 °C.

Formation of a complex between LamB trimers and His_6−gpJ was confirmed by Western blots with antibodies against the His_6 tag. Figure 11 demonstrates that His_6−gpJ (lane 1) could be visualized using these antibodies but not WT LamB (lane 2) or the LamB Δ4+Δ6+Δ9v mutant (lane 3). Lane 4 shows that the antibody detected the LamB−His_6−gpJ complex. The complex was absent when both proteins were boiled (lane 5). Similarly, the antibody was able to visualize the complex between LamB Δ4+Δ6+Δ9v and His_6−gpJ (lane 6), but not when the proteins were boiled (lane 7). Essential for complex formation was the native form of LamB, i.e., the trimers. When His_6−gpJ was boiled but not LamB, the complexes could be detected (see Figure 11, lane 8), but they were absent when LamB was boiled but not His_6−gpJ (lane 9). Similar results were obtained for LamB of *S. sonnei* (data not shown). Taken together, the results represent additional proof for the interaction of WT LamB and LamB Δ4+Δ6+Δ9v with His_6−gpJ.

DISCUSSION

MBP−gpJ and His_6−gpJ Exhibit a High Binding Affinity for LamB. The C-terminal part (amino acids 684−1131) of the J protein from the tail of phage Lambda called gpJ is sufficient for binding to LamB (*22*). MBP (MalE) is a periplasmic protein, which binds carbohydrates with high affinity. Its presence confers the periplasmic space to a sink for carbohydrates and allows their vectorial transport across the outer membrane (*66*). Furthermore, MBP is involved in the transport of maltose and maltooligosaccharides across the bacterial inner membrane where it interacts with the MalF−MalG−$MalK_2$ complex (*29*). Earlier investigations had shown that MBP may interfere with the properties of LamB (*62*). However, control experiments performed here and elsewhere demonstrated that MBP is not able to modify the properties of LamB in vivo and in vitro (*28*, *63*). Furthermore, no binding of MBP to the periplasmic side of LamB was found in vivo by electronic microscopy of *E. coli* cells using an anti-MBP antibody and in vitro by immunodetection (*46*). The binding of MBP−gpJ to LamB has

nothing to do with a direct interaction between LamB and MBP because there is no evidence of binding of the MBP protein to the periplasmic side of LamB. This means that the binding of MBP−gpJ to LamB is definitely caused by the gpJ moiety of the chimera protein.

His_6−gpJ also has a high affinity for LamB. First, the interaction of LamB with His_6−gpJ seemed to block channel reconstitution, probably because binding of a large hydrophilic moiety to LamB hinders its reconstitution. Second, we demonstrated that preincubation of reconstituted LamB with His_6−gpJ did not allow MBP−gpJ-mediated channel block. Only at a very high MBP−gpJ concentration (higher than that of His_6−gpJ) was some decrease in LamB-mediated membrane conductance observed, an indication of some competition between His_6−gpJ and MBP−gpJ for the binding site at the cis side of the LamB channel. Finally, SDS−PAGE of the LamB−MBP−gpJ complex as well as with LamB−His_6−gpJ mixtures demonstrates the formation of oligomers on the gels, which were also detected by antibodies against MBP and the His_6 tag in Western blots. The complexes were not sensitive for the heating of His_6−gpJ, but they were absent when the LamB trimers were heated and dissociated. The formation of LamB−MBP−gpJ complexes and of those between His_6−gpJ and LamB indicates that the stability constant for complex formation was very high. It is noteworthy that the complexes withstand migration for ∼2 h in the electric field during the run of SDS−PAGE.

MBP−gpJ and His_6−gpJ Bind to the Surface-Exposed Side of the LamB Channel. The experimental data reveal a clearly asymmetric effect of the MBP−gpJ protein on LamB-mediated membrane conductance. MBP−gpJ added to the cis side of the membrane caused a dramatic decrease in conductance. MBP−gpJ added to the trans side resulted in an only negligible decrease. This result suggested that MBP−gpJ bound preferentially to the side of LamB, which is exposed to the cis side. The orientation of LamB in reconstitution experiments using planar lipid bilayers was a matter of debate. Experiments with phage Lambda and single-channel analysis of carbohydrate transport suggested that the cell surface-exposed side points to the trans side, as it is the in vivo situation (*57*, *67*). On the other hand, studies with loop deletion mutants, the interaction of phage Lambda with LamB, the effect of low pH on channel closure, and the use of asymmetric substrates suggested that the surface-exposed side of LamB (i.e., the loops) is localized on the cis side of the membrane (*47*, *56*, *57*, *68*). The latter orientation appears to be more likely when the high energy that is needed to move the long surface-exposed (and hydrophilic) loops through the hydrocarbon core of the lipid bilayer membrane during reconstitution is considered. The binding of MBP−gpJ to the cell surface-exposed part of LamB agrees very well with such an orientation because it is known that MBP−gpJ binds to the surface of the *E. coli* cells (*22*, *46*). Similarly, His_6−gpJ also binds to the cis side of the reconstituted LamB channels, where amino acids of several surface-exposed loops are involved in phage binding (*31*, *33*−*35*, *47*, *69*, *70*). Taken together, the C-terminal fragment of the J protein from the phage tail interacts with the surface-exposed side of LamB.

MBP−gpJ and His_6−gpJ Are Not Channel-Forming Components. Phage T1 has two genes (*orf26* and *orf33*) specifying proteins with homology to tail fibers (*71*). Protein p33 of phage T1 and protein J of phage Lambda share some sequence similarity (i.e., ∼25% amino acid identity). Similarly, pb2 of phage T5 shares ∼12% sequence identity with protein J and p33. This could mean that MBP−gpJ and His_6−gpJ are channel formers because it has been demonstrated that pb2 is a channel-forming component (*60*). However, strikingly, there is not much homology between the C-terminal portions of the two proteins: from residues 888 of J and 897 of p33 (J is 1132 residues in length and p33 is 1172). On the other hand, we have provided strong evidence that the 100 C-terminal residues of J are critical for the recognition of and adsorption to LamB (*22*, *46*). Single-amino acids substitutions in the last C-terminal residues of J were sufficient to abolish LamB recognition (*46*). Moreover, we have shown that such mutations could be suppressed by mutations in surface loops of LamB (*70*). It is thus most likely that J is the only phage protein responsible for LamB recognition and binding. Recognition of surface receptors and binding in the case of the T1 and T5 phages are different compared to those of phage Lambda. Phage T5 possesses two types of tail fibers, three L-shaped (LTF) and one central, straight tail fiber (STF) (*72*, *73*). Binding of T5 to FhuA is mediated by tail protein pb5 which is not located at the tip of the tail fiber. The STF, formed by approximately six copies of tail protein pb2, does not mediate binding to FhuA but is involved in the penetration of T5 DNA through the *E. coli* cell envelope [as suggested by the pore forming activity of pb2 (*60*)]. Furthermore, the interaction between phage Lambda and LamB is presumably completely different because of the structures of the receptors. LamB is a trimeric protein (*16*, *17*), while FhuA, BtuB, and other TonB-dependent OM transporters are monomeric proteins (*19*, *20*). These proteins are very similar in basic structure; their membrane-spanning portion consists of a barrel with 22 antiparallel amphipathic β-strands, and the pore of the barrel is occluded by insertion of a conserved N-terminal globular domain (the cork), which opens when FhuA interacts with the phage tail (*74*). Considering the structural differences between the outer membrane transporters and LamB and between phage Lambda and the T1 and T5 phages and considering the experimental observations of this study, it is rather unlikely that MBP−gpJ or His_6−gpJ is a channel-forming component.

The Binding of MBP−gpJ to LamB but Not That of His_6−gpJ Blocks the Channel for Passage of Ions. Titration of LamB-mediated conductance led to a complete block of the channel for ion flux in single-channel experiments. Surprisingly, channel block by MBP−gpJ occurred in a single step despite the fact that the conductance of a single LamB channel is that of a trimer. Carbohydrates block the conductance of a LamB channel in three individual steps (*57*). This could mean that the gpJ part of MBP−gpJ (molecular mass of ∼97 kDa) binds to a single channel but that the MBP part is bulky enough to cause channel closure of all three channels in a trimer. The binding of gpJ to the trimer and not to a monomer appears to be more likely because MBP−gpJ-mediated closing of LamB is a single-hit process (see below). His_6−gpJ alone (molecular mass of ∼50 kDa) is presumably not bulky enough to block the three channels in a LamB trimer. It is also possible that His_6−gpJ has a more superficial association with the LamB loops than does

MBP−gpJ. SDS−PAGE and Western blots of LamB−MBP−gpJ and LamB−His_6−gpJ complexes provide an additional indication of such a possibility because MBP−gpJ bound to only the LamB trimers and not to the monomers. Furthermore, SDS−PAGE and Western blots demonstrate that only one MBP−gpJ or one His_6−gpJ binds to the LamB trimers.

The binding place for gpJ is presumably the central part of the trimer. Such an arrangement for the LamB−gpJ complex could also explain why His_6−gpJ obviously binds to LamB but why binding does not result in channel closure for the flux of ions because the diameter of His_6−gpJ is not sufficient for the complete block of LamB trimers for ion conduction. This cannot be understood if three His_6−gpJ molecules (molecular mass of ∼50 kDa each) bind to the external surface of the LamB trimers. It is noteworthy that the LamB−His_6−gpJ complex did not show any interference with maltopentaose binding, a molecule that is larger than potassium or chloride ions. This was shown by titration experiments with maltopentaose added to the cis side of reconstituted LamB mutant Y118G channels treated before with 100 nM His−gpJ. Taken together, it seems likely that the complex between LamB and MBP−gpJ or His_6−gpJ is a 1/1 complex. The results presented here for the interaction of His_6−gpJ with LamB agree with binding of the entire Lambda phage to LamB reconstituted in bilayer experiments, which did not modify the conductance of LamB (*69*).

The Half-Saturation Constant for Binding of MBP−gpJ and His_6−gpJ to LamB Is in the Nanomolar Range. The titration experiments of LamB-mediated membrane conductance with MBP−gpJ allowed calculation of the stability constant for binding to LamB using a simple model (*28*). The single problem for the use of the model was that the LamB-mediated conductance was not completely shut down in the titration experiments. Closure of all channels reached on average only ∼85% of the open channel conductance. This problem was taken into account using eq 5, which resulted in a small change in the stability constant. The reason the LamB channels did not completely close in the multichannel experiments is presumably related to the orientation of the reconstituted LamB channels. In previous papers, we could demonstrate that the cell surface-exposed side (i.e., the loops) of reconstituted LamB channels is oriented by 80−90% to the cis side of the membrane (*47*, *56*). This means that ∼10−20% of the LamB channels do not respond to the addition of MMB−gpJ to the cis side of the membrane as they have an opposite orientation with the receptor side exposed to the trans side of the membrane. The incomplete closure of LamB in the titration experiments has definitely nothing to do with impurities in the protein samples. The use of the starch column for affinity purification of the different LamB and LamB mutant proteins provided pure proteins without any indication of contaminants. Binding of phage Lambda to the cell surfaces can be influenced by the ionic strength and the concentration of the Mg^{2+} ions (*64*, *75*). Interestingly, this parameter had no effect on the complex between LamB and MBP−gpJ, which suggests that additional interactions are also involved in binding of phage Lambda to the *E. coli* cells. In particular, it is possible that Mg^{2+} stabilizes complex formation in the presence of LPS that is not present in the lipid bilayer experiments.

The evidence for binding of His_6−gpJ to LamB in a concentration range similar to that for MBP−gpJ is more indirect because no channel closure could be observed. Nevertheless, it is obvious from the experiments in which LamB channels were preincubated with His_6−gpJ and an only insignificant effect of MBP−gpJ was observed that the half-saturation constant of His_6−gpJ binding is also in the nanomolar range. When the results of Figure 9 and of similar experiments are considered, it seems to be possible that the binding of His_6−gpJ to LamB has a half-saturation constant even smaller than that of MBP-gpJ. The degree of channel block at 155 nM MBP−gpJ was still less than 50% of the total number of channels, which means that 100 nM His_6−gpJ occupies more than 50% of the LamB channels, which suggests indeed a lower half-saturation constant for binding of His_6−gpJ to LamB than for MBP−gpJ binding.

Amino Acids of External Loops L4 and L6 and Part of Loop L9 Are Not Alone Responsible for gpJ Binding. Formation of a complex was also possible between the LamB Δ4+Δ6+Δ9v mutant and MBP−gpJ or His−gpJ. This was shown by SDS−PAGE, Western blots, and bilayer experiments in which MBP−gpJ blocked ion conductance through the LamB Δ4+Δ6+Δ9v mutant. This result is in some contrast to the results of in vivo experiments in which loops L4, L6, and L9 are necessary for in vivo binding of phage Lambda to LamB. Their deletion should influence binding of MBP−gpJ and His_6−gpJ to LamB. However, we showed in a previous publication (*47*) that loops L4, L6, and L9 are not involved in the in vitro transport of carbohydrates through LamB. This contradicts in vivo transport of carbohydrates through the LamB loop deletion mutants, where the rate of transport is decreased (*47*). This was explained by the assumption that LPS blocks partially the LamB channels when the major surface-exposed loops are removed; i.e., the O antigen side chains hinder access of carbohydrates to the mutant channels. This also means that LPS side chains could also block in such a case access of the phage tail to LamB loop deletion channels, which could explain the difference between the in vivo and in vitro experiments.

The binding of MBP−gpJ and His_6−gpJ to the loop deletion mutant also offers other interesting insight into the interaction between gpJ and LamB. Amino acids of the LamB protein involved in binding of the bacteriophage Lambda have been investigated for many years by site-directed mutagenesis. These experiments resulted in phage resistant mutants with a variable efficiency, called class I mutants. The mutations on the LamB gene that allow this phenotype are located on outer loops L1, L4, L6, and L9. Class I mutants block growth of WT Lambda host range (λh^+). Extended host range phage mutants (λh) can also bind to class I LamB proteins and infect the cells. Two-step extended host range mutants (λhh^*) can also bind to class II LamB and restore its infection activity. All these amino acids involved in class I and class II LamB mutants are localized on outer loops L4, L6, and L9 (*31*−*35*, *47*, *70*, *76*). However, the identified amino acids on the surface-exposed loops are not alone essential for the binding of the gpJ protein, although they are essential for the infection of the cells with bacteriophage Lambda. This means that the other amino acids forming the binding site for gpJ may be localized somewhere on the surface of its barrel structure, possibly in the center of the LamB trimers.

ACKNOWLEDGMENT

We are grateful to Christian Andersen for helpful discussions.

REFERENCES

1. Smit, J., Kamio, Y., and Nikaido, H. (1975) Outer membrane of *Salmonella typhimurium*: Chemical analysis and freeze-fracture studies with lipopolysaccharide mutants, *J. Bacteriol. 124*, 942−958.
2. Kamio, Y., and Nikaido, H. (1976) Outer membrane of *Salmonella typhimurium*: Accessibility of phospholipid head groups to phospholipase c and cyanogen bromide activated dextran in the external medium, *Biochemistry 15*, 2561−2570.
3. Nikaido, H., and Vaara, M. (1985) Molecular basis of bacterial outer membrane permeability, *Microbiol. Rev. 49*, 1−32.
4. Nikaido, H. (2003) Molecular basis of bacterial outer membrane permeability revisited, *Microbiol. Mol. Biol. Rev. 67*, 593−656.
5. Letellier, L., Boulanger, P., Plancon, L., Jacquot, P., and Santamaria, M. (2004) Main features on tailed phage, host recognition and DNA uptake, *Front. Biosci. 9*, 1228−1339.
6. Letellier, L., Plançon, L., Bonhivers, M., and Boulanger, P. (1999) Phage DNA transport across membranes, *Res. Microbiol. 150*, 499−505.
7. Brussow, H., and Hendrix, R. W. (2002) Phage genomics: Small is beautiful, *Cell 108*, 13−16.
8. Hendrix, R. W. (2003) Bacteriophage genomics, *Curr. Opin. Microbiol. 6*, 506−511.
9. Weinbauer, M. G. (2004) Ecology of prokaryotic viruses, *FEMS Microbiol. Rev. 28*, 127−128.
10. Chibani-Chennoufi, S., Bruttin, A., Dillmann, M. L., and Brussow, H. (2004) Phage-host interaction: An ecological perspective, *J. Bacteriol. 186*, 3677−3686.
11. Sutherland, I. W., Hughes, K. A., Skillman, L. C., and Tait, K. (2004) The interaction of phage and biofilms, *FEMS Microbiol. Lett. 232*, 1−6.
12. Nikaido, H. (1992) Porins and specific channels of bacterial outer membranes, *Mol. Microbiol. 6*, 435−442.
13. Benz, R., and Bauer, K. (1988) Permeation of hydrophilic molecules through the outer membrane of Gram-negative bacteria. Review on bacterial porins, *Eur. J. Biochem. 176*, 1−19.
14. Weiss, M. S., Abele, U., Weckesser, J., Welte, W., Schiltz, E., and Schulz, G. E. (1991) Molecular architecture and electrostatic properties of a bacterial porin, *Science 254*, 1627−1630.
15. Cowan, S. W., Schirmer, T., Rummel, G., Steiert, M., Gosh, R., Pauptit, R. A., Jansonius, J. N., and Rosenbusch, J. P. (1992) Crystal structures explain functional properties of two *E. coli* porins, *Nature 356*, 727−733.
16. Schirmer, T., Keller, T., Wang, Y., and Rosenbusch, J. P. (1995) Structural basis for sugar translocation through maltoporin channels at 3.1 Å resolution, *Science 267*, 512−514.
17. Dutzler, R., Wang, Y. F., Rizkallah, P., Rosenbusch, J. P., and Schirmer, T. (1996) Crystal structures of various maltooligosaccharides bound to maltoporin reveal a specific sugar translocation pathway, *Structure 4*, 127−134.
18. Ferguson, D., Hofmann, E., Coulton, J. W., Diederichs, K., and Welte, W. (1998) Siderophore-mediated iron transport: Crystal structure of FhuA with bound lipopolysaccharide, *Science 282*, 2215−2220.
19. Locher, K. P., Rees, B., Koebnik, R., Mitschler, A., Moulinier, L., Rosenbusch, J. P., and Moras, D. (1998) Transmembrane signaling across the ligand-gated FhuA receptor: Crystal structures of free and ferrichrome-bound states reveal allosteric changes, *Cell 95*, 771−778.
20. Chimento, D. P., Mohanty, A. K., Kadner, R. J., and Wiener, M. C. (2003) Substrate-induced transmembrane signaling in the cobalamin transporter BtuB, *Nat. Struct. Biol. 10*, 394−401.
21. Randall-Hazelbauer, L., and Schwartz, M. (1973) Isolation of the bacteriophage lambda receptor from *Escherichia coli*, *J. Bacteriol. 116*, 1436−1446.
22. Wang, J., Michel, V., Hofnung, M., and Charbit, A. (1998) Cloning of the J gene of bacteriophage Lambda, expression and solubilization of the J protein: First *in vitro* studies on the interactions between J and LamB, its cell surface receptor, *Res. Microbiol. 149*, 611−624.
23. Bonhivers, M., Ghazi, A., Boulanger, P., and Letellier, L. (1996) FhuA, a transporter of the *Escherichia* coli outer membrane, is converted into a channel upon binding of bacteriophage T5, *EMBO J. 15*, 1850−1856.
24. Plancon, L., Janmot, C., le Maire, M., Desmadril, M., Bonhivers, M., Letellier, L., and Boulanger, P. (2002) Characterization of a high-affinity complex between the bacterial outer membrane protein FhuA and the phage T5 protein pb5, *J. Mol. Biol. 318*, 557−569.
25. Szmelcman, S., and Hofnung, M. (1975) Maltose transport in *Escherichia coli* K-12: Involvement of the bacteriophage lambda receptor, *J. Bacteriol. 124*, 112−118.
26. Palva, E. T. (1978) Major outer membrane protein in *Salmonella typhimurium* induced by maltose, *J. Bacteriol. 136*, 286−294.
27. Bloch, M. A., and Desaymard, C. (1985) Antigenic polymorphism of the LamB protein among members of the family *Enterobacteriaceae*, *J. Bacteriol. 163*, 106−110.
28. Benz, R., Schmid, A., Nakae, T., and Vos Scheperkeuter, G. H. (1986) Pore formation by LamB of *Escherichia coli* in lipid bilayer membranes, *J. Bacteriol. 165*, 978−986.
29. Boos, W., and Shuman, H. (1998) Maltose/maltodextrin system of *Escherichia coli*: Transport, metabolism, and regulation, *Microbiol. Mol. Biol. Rev. 62*, 204−229.
30. Charbit, A. (2003) Maltodextrin transport through LamB, *Front. Biosci. 8*, 265−274.
31. Charbit, A., Clement, J. M., and Hofnung, M. (1984) Further sequence analysis of the phage lambda receptor site. Possible implications for the organization of the LamB protein in *Escherichia coli* K12, *J. Mol. Biol. 175*, 395−401.
32. Hofnung, M., Jezierska, A., and Braun-Breton, C. (1976) LamB mutations in *Escherichia coli* K12: Growth of lambda host range mutants and effect of nonsense suppressors, *Mol. Gen. Genet. 145*, 207−213.
33. Clement, J. M., Lepouce, E., Marchal, C., and Hofnung, M. (1983) Genetic study of a membrane protein: DNA sequence alterations due to 17 LamB point mutations affecting adsorption of phage lambda, *EMBO J. 2*, 77−80.
34. Gehring, K., Charbit, A., Brissaud, E., and Hofnung, M. (1987) Bacteriophage lambda receptor site on the *Escherichia coli* K-12 LamB protein, *J. Bacteriol. 169*, 2103−2106.
35. Charbit, A., Werts, C., Michel, V., Klebba, P., Quillardet, P., and Hofnung, M. (1994) A role for residue 151 of LamB in bacteriophage lambda adsorption: Possible steric effect of amino acid substitutions, *J. Bacteriol. 176*, 3204−3209.
36. Friedman, D. I., and Court, D. L. (2001) Bacteriophage lambda: Alive and well and still doing its thing, *Curr. Opin. Microbiol. 4*, 201−207.
37. Hendrix, R., Roberts, J., Stahl, F., and Weisberg, R. (1983) *Lambda II*, Cold Spring Harbor Laboratory Press, Plainview, NY.
38. Sambrook, J., Fritsch, E. F., and Maniatis, T. (1989) *Molecular Cloning: A Laboratory Manual*, Cold Spring Harbor Laboratory Press, Plainview, NY.
39. Hoess, R. H. (2002) Bacteriophage lambda as a vehicle for peptide and protein display, *Curr. Pharm. Biotechnol. 3*, 23−28.
40. Merril, C. R., Biswas, B., Carlton, R., Jensen, N. C., Creed, G. J., Zullo, S., and Adhya, S. (1996) Long-circulating bacteriophage as antibacterial agents, *Proc. Natl. Acad. Sci. U.S.A. 93*, 3188−3192.
41. Duckworth, D. H., and Gulig, P. A. (2002) Bacteriophages: Potential treatment for bacterial infections, *BioDrugs 16*, 57−62.
42. Projan, S. (2004) Phage-inspired antibiotics? *Nat. Biotechnol. 22*, 167−168.
43. Roa, M., and Scandella, D. (1976) Multiple steps during the interaction between coliphage lambda and its receptor protein *in vitro*, *Virology 72*, 182−194.
44. Roessner, C. A., Struck, D. K., and Ihler, G. M. (1983) Injection of DNA into liposomes by bacteriophage Lambda, *J. Biol. Chem. 258*, 643−648.
45. Roessner, C. A., Struck, D. K., and Ihler, G. M. (1983) Morphology of complexes formed between bacteriophage Lambda and structures containing the Lambda receptor, *J. Bacteriol. 153*, 1528−1534.
46. Wang, J., Hofnung, M., and Charbit, A. (2000) The C-terminal portion of the tail fiber protein of bacteriophage lambda is responsible for binding to LamB, its receptor at the surface of *Escherichia coli* K-12, *J. Bacteriol. 182*, 508−512.
47. Andersen, C., Bachmeyer, C., Tauber, H., Benz, R., Wang, J., Michel, V., Newton, S. M., Hofnung, M., and Charbit, A. (1999) In vivo and in vitro studies of major surface loop deletion mutants of the *Escherichia coli* K-12 maltoporin: Contribution to maltose

and maltooligosaccharide transport and binding, *Mol. Microbiol. 32*, 851−867.
48. Orlik, F., Andersen, C., and Benz, R. (2002) Site-directed mutagenesis of tyrosine 118 within the central constriction site of the LamB (Maltoporin) channel of *Escherichia coli*. I. Effect on ion transport, *Biophys. J. 82*, 2466−2475.
49. Klebba, P. E., Hofnung, M., and Charbit, A. (1994) A model of maltodextrin transport through the sugar-specific porin, LamB, based on deletion analysis, *EMBO J. 13*, 4670−4675.
50. Benz, R., Janko, K., Boos, W., and Läuger, P. (1978) Formation of large, ion-permeable membrane channels by the matrix protein (porin) of *Escherichia coli*, *Biochim. Biophys. Acta 511*, 305−319.
51. Benz, R., Schmid, A., and Vos-Scheperkeuter, G. H. (1987) Mechanism of sugar transport through the sugar-specific LamB-channel of *Escherichia coli* outer membrane, *J. Membr. Biol. 100*, 12−29.
52. Nekolla, S., Andersen, C., and Benz, R. (1994) Noise analysis of ion current through the open and the sugar-induced closed state of the LamB-channel of *Escherichia coli* outer membrane: Evaluation of the sugar binding kinetics to the channel interior, *Biophys. J. 66*, 1388−1397.
53. Jordy, M., Andersen, C., Schülein, K., Ferenci, T., and Benz, R. (1996) Rate constants of sugar transport through two LamB mutants of *Escherichia coli*: Comparison to wild-type maltoporin and to LamB of *Salmonella typhimurium*, *J. Mol. Biol. 259*, 666−678.
54. Bachmeyer, C., Benz, R., Barth, H., Aktories, K., Gilbert, M., and Popoff, M. R. (2001) Interaction of *Clostridium botulinum* C2 toxin with lipid bilayer membranes and Vero cells: Inhibition of channel function by chloroquine and related compounds *in vitro* and intoxification in vivo, *FASEB J. 15*, 1658−1660.
55. Andersen, C., Jordy, M., and Benz, R. (1995) Evaluation of the rate constants of sugar transport through maltoporin (LamB) of *Escherichia coli* from the sugar-induced current noise, *J. Gen. Physiol. 105*, 385−401.
56. Andersen, C., Schiffler, B., Charbit, A., and Benz, R. (2002) Ph-induced collapse of the extracellular loops closes *Escherichia coli* maltoporin and allows the study of asymmetric sugar binding, *J. Biol. Chem. 277*, 41318−41325.
57. Kullman, L., Winterhalter, M., and Bezrukov, S. M. (2002) Transport of maltodextrins through maltoporin: A single-channel study, *Biophys. J. 82*, 803−812.
58. Wohnsland, F., and Benz, R. (1997) 1/f-Noise of open bacterial porin channels, *J. Membr. Biol. 158*, 77−85.
59. Bezrukov, S. M., and Winterhalter, M. (2000) Examining noise sources at the single-molecule level: 1/f noise of an open maltoporin channel, *Phys. Rev. Lett. 85*, 202−205.
60. Feucht, A., Schmid, A., Benz, R., Schwarz, H., and Heller, K. J. (1990) Pore formation associated with the tail-tip protein pb2 of bacteriophage T5, *J. Biol. Chem. 265*, 18561−18567.
61. Schülein, K., Schmid, K., and Benz, R. (1991)The sugar-specific outer membrane channel ScrY contains functional characteristics of general diffusion pores and substrate-specific porins, *Mol. Microbiol. 5*, 2233−2241.
62. Neuhaus, J. M., Schindler, H., and Rosenbusch, J. P. (1983) The periplasmic maltose-binding protein modifies the channel-forming characteristics of maltoporin, *EMBO J. 2*, 1987−1991.
63. Brass, J. M., Bauer, K., Ehmann, U., and Boos, W. (1985) Maltose-binding protein does not modulate the activity of maltoporin as a general porin in *Escherichia coli*, *J. Bacteriol. 161*, 720−726.
64. Schwartz, M. (1976) The adsorption of coliphage Lambda to its host: Effect of variations in the surface density of receptor and in phage-receptor affinity, *J. Mol. Biol. 103*, 521−536.
65. Katsura, I. (1976) Isolation of lambda prophage mutants defective in structural genes: Their use for the study of bacteriophage morphogenesis, *Mol. Gen. Genet. 148*, 31−42.
66. Benz, R., and Orlik, F. (2004) Functional reconstitution and properties of specific porins, in *Prokaryotic and Eukaryotic Porins: Structure, Function, Mechanisms* (Benz, R., Ed.) pp 183−212, Wiley-VCH Verlag GmbH, Weinheim, Germany.
67. Van Gelder, P., Dumas, F., and Winterhalter, M. (2000) Understanding the function of bacterial outer membrane channels by reconstitution into black lipid membranes, *Biophys. Chem. 85*, 153−167.
68. Danelon, C., Brando, T., and Winterhalter, M. (2003) Probing the orientation of reconstituted maltoporin channels at a single molecular level, *J. Biol. Chem. 278*, 35542−35551.
69. Berrier, C., Bonhivers, M., Letellier, L., and Ghazi, A. (2000) High-conductance channel induced by the interaction of phage lambda with its receptor maltoporin, *FEBS Lett. 476*, 129−133.
70. Werts, C., Michel, V., Hofnung, M., and Charbit, A. (1994) Adsorption of bacteriophage Lambda on the LamB protein of *Escherichia coli* K-12: Point mutations in gene J of Lambda responsible for extended host range, *J. Bacteriol. 176*, 941−947.
71. Roberts, M. D., Martin, N. L., and Kropinski, A. M. (2004) The genome and proteome of coliphage T1, *Virology 318*, 245−266.
72. Mondigler, M., Vogele, R. T., and Heller, K. J. (1995) Overproduced and purified receptor binding protein pb5 of bacteriophage T5 binds to the T5 receptor protein FhuA, *FEMS Microbiol. Lett. 130*, 293−300.
73. Mondigler, M., Holz, T., and Heller, K. J. (1996) Identification of the receptor-binding regions of pb5 proteins of bacteriophages T5 and BF23, *Virology 219*, 19−28.
74. Bonhivers, M., Ghazi, A., Boulanger, P., and Letellier, L. (1996) FhuA, a transporter of the *Escherichia* coli outer membrane, is converted into a channel upon binding of bacteriophage T5, *EMBO J. 15*, 1850−1856.
75. Schwartz, M. (1975) Reversible interaction between coliphage Lambda and its receptor protein, *J. Mol. Biol. 99*, 185−201.
76. Dargent, B., Charbit, A., Hofnung, M., and Pattus, F. (1988) Effect of point mutations on the in-vitro pore properties of maltoporin, a protein of *Escherichia coli* outer membrane, *J. Mol. Biol. 201*, 497−506.

BI051800V